Inorganic Chemistry

Article

pubs.acs.org/IC

Synthesis and Characterization of Amine-Functionalized Mixed-Ligand Metal–Organic Frameworks of UiO-66 Topology

Sachin M. Chavan,*[,†] Greig C. Shearer,[†] Stian Svelle,[†] Unni Olsbye,[†] Francesca Bonino,[‡] Jayashree Ethiraj,[‡] Karl Petter Lillerud,[†] and Silvia Bordiga*[,†,‡]

[†]inGAP Center of Research Based Innovation, Department of Chemistry, University of Oslo, P.O. Box 1033, Blindern, 0315 Oslo, Norway

[‡]Department of Chemistry, NIS and INSTM Reference Centre, University of Turin, Via G. Quarello 15 I-10135 Torino, Italy

Supporting Information

ABSTRACT: A series of amine-functionalized mixed-linker metal–organic frameworks (MOFs) of idealized structural formula $Zr_6O_4(OH)_4(BDC)_{6-6X}(ABDC)_{6X}$ (where BDC = benzene-1,4-dicarboxylic acid, ABDC = 2-aminobenzene-1,4-dicarboxylic acid) has been prepared by solvothermal synthesis. The materials have been characterized by thermogravimetric analysis (TGA), powder X-ray diffraction (PXRD), and Fourier transform infrared (FTIR) spectroscopy with the aim of elucidating the effect that varying the degrees of amine functionalization has on the stability (thermal and chemical) and porosity of the framework. This work includes the first application of ultraviolet–visible light (UV-vis) spectroscopy in the quantification of ABDC in mixed-linker MOFs.

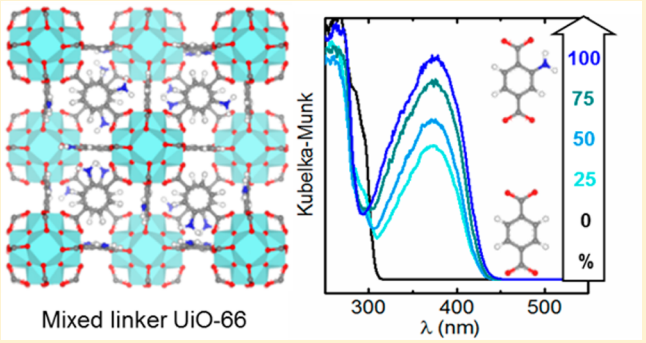

1. INTRODUCTION

Metal–organic frameworks (MOFs) are crystalline materials that are comprised of metal ions or clusters coordinated to often-rigid organic molecules, forming three-dimensional porous structures.[1−4] This combination of inorganic and organic building blocks gives rise to near infinite structural and chemical possibilities. Such potential has resulted in these materials generating great interest in gas separation/storage,[5,6] catalysis,[7−9] and drug delivery[10,11] applications. One emerging area that opens yet more possibilities is Post-Synthetic Modification (PSM).[12,13] To this end, the basicity and reactivity of pendant $-NH_2$ groups has resulted in amine-functionalized MOFs being the most often exploited materials for this purpose.[14−17] Moreover, many amine-functionalized MOFs have shown improved CO_2 uptake[18−20] versus their non-functionalized, isostructural analogues. Designing MOFs with tailored functional sites is the pathway to develop materials for advanced applications. However, often it has been found that fully functionalized materials are thermally less stable; imposing challenges in solvent removal and activation of the framework.[15,21] In order to circumvent this problem, it has recently been shown that diluting the extent of functionalization via a "mixed linker" (ML) approach is effective tuning the stability of the material.[22−25] Furthermore, varying the composition of mixed-linker MOFs can result in systematic alteration of the gas adsorption capacity and selectivity of the material. Such an approach has been previously been adopted on several MOF topologies, namely MOF-5,[26] MIL-53-Al,[27,28] CAU-10,[29] and MIL-101,[30] where a mixture of benzene-1,4-dicarboxylic acid (BDC) and its amino-, bromo-, nitro-, and methyl-functionalized derivatives were used as linkers. In these studies, various properties of the materials were significantly influenced by the amount and type of functionality introduced into the framework; namely, the surface area (MOF-5),[26] the breathing pressure (MIL-53),[28] and sorption properties (CAU-10)[29] were observed to have been affected. In order to design mixed-linker MOFs for a particular purpose, it is important to first gain an understanding of how the properties of the materials are affected by altering the ratio between the linkers. To allow such correlations to be made, mixed-linker MOFs with varying degrees of functionalization must be synthesized and thoroughly characterized.

UiO-66,[31−34] which is a Zr(IV)-based MOF, has recently received great interest, because of its high thermal and chemical stability. In accordance with observations on other framework types, UiO-66-NH_2, the fully amino functionalized isostructural analogue, is thermally less stable than unmodified UiO-66.[15] Moreover, post-synthetic modification of UiO-66-NH_2 can be challenging, because of the steric hindrance imposed by the large density of pendant $-NH_2$ groups pointing into the cavities.[35−37] The desired $-NH_2$ content may thus vary depending on the application, i.e., it may be beneficial to maximize $-NH_2$ loading for the carbon capture and storage applications, whereas a more diluted $-NH_2$ loading might be

Received: March 15, 2014
Published: August 22, 2014

   dx.doi.org/10.1021/ic500607a | Inorg. Chem. 2014, 53, 9509−9515

preferred from a post-synthetic modification and catalysis point of view.

The only existing study on amine-based mixed-linker MOFs of the UiO-66 topology was reported by Kim et al.,[38] where a mixture of amino- and bromo-functionalized BDC was used to form UiO-66-Br-NH_2, which is a MOF that was found to be more thermally stable than UiO-66-NH_2. Moreover, selective post-synthetic modification of these functional groups in mixed-linker MOFs was demonstrated.

In this contribution, we present the synthesis and characterization of mixed-linker MOFs of the UiO-66 framework topology, prepared using a mixture of BDC and 2-aminobenzene-1,4-dicarboxylic acid (ABDC). The series of samples has been characterized for their thermal and chemical stability, ease of activation, and porosity. Following the use of an original digestion method (OH^--based media instead of F^--based media), the ABDC content of the MOFs was quantified by UV-vis spectroscopy for the first time, with the results validated by the more conventional ^{1}H NMR method.

2. MATERIALS AND METHODS

2.1. Material Synthesis. All chemicals were obtained from commercial vendors and used without further purification. The reaction mixtures were prepared in a volumetric flask by sequentially adding *N*,*N*-dimethylformamide, $ZrCl_4$, H_2O, and linker, and in a 350:1:1.3:1 molar ratio at room temperature. The linker portion consisted of five different mixtures of BDC and ABDC, resulting in five different materials. Specifically, the molar fractions of ABDC with respect to BDC were: 0, 0.25, 0.50, 0.75, and 1. The five resulting materials are hereafter labeled UiO-66, UiO-66-NH_2-25, UiO-66-NH_2-50, UiO-66-NH_2-75, and UiO-66-NH_2, respectively. See Table S1 in the Supporting Information for the masses of the synthesis reagents. The flasks were then sealed and placed in an oven at 100 °C where the synthesis was performed under static conditions for 72 h. The resulting products precipitated as microcrystalline powders which were then separated from the solution by centrifugation and washed three times in DMF (40 mL). Water exchanged samples were obtained by washing the materials three times in excess of water at 80 °C for 2 h. Finally, all the samples were dried at 60 °C in air for 24 h. All syntheses were successfully reproduced and resulted in a 90−95% yield of MOF material. In a parallel study by our group, the UiO-66 synthesis conditions have been optimized in order to limit the number of missing linkers. A second set of mixed ligand BDC/ABDC UiO-66 samples has been synthesized based on this method and is described in section G of the Supporting Information.

2.2. Methods. *2.2.1. Physicochemical Characterization.* Powder X-ray diffraction (PXRD) patterns were collected on a Bruker D8 Discovery diffractometer equipped with a focusing Ge-monochromator, using Cu Kα1 radiation (1.5418 Å) and a Bruker LYNXEYE detector. PXRD were collected in reflectance Bragg−Brentano geometry in the 2θ range from 3° to 50°. Thermogravimetric analysis (TGA) was performed on typically ca. 25−30 mg of powdered sample loaded inside a platinum crucible on a Stanton Redcroft TG-DSC instrument. Samples were heated at a ramp 5 °C per minute to 700 °C; under the flow of N_2 and O_2 with flow rates 20 and 5 mL per minute, respectively. Nitrogen sorption measurements were performed on a BelSorb mini II instrument at 77 K. Prior to adsorption measurements samples were pretreated (activated) under vacuum for 1 h at 80 °C and 2 h at 200 °C. Brunauer−Emmett−Teller (BET) and Langmuir surface areas were calculated by fitting the isotherm data in the p/p_0 range of 0−0.1. The chemical stability of the MOFs was evaluated by suspending the samples in water (RT for 1 month, 100 °C for 24 h), 1 M HCl (24 h), and 1 M NaOH (24 h) in separate experiments. To confirm the framework stability, PXRD spectra were measured before and after the chemical treatment for each sample.

2.2.2. Quantitative Analysis of Linker. Prior to measurement, MOF samples were digested by adding a weighed amount of sample (10−20 mg for UV-vis, 20 mg for ^{1}H NMR) to a 1 M NaOH−H_2O solution (for UV−vis), and 600 μL of a 1 M NaOH−D_2O solution (for ^{1}H NMR) and allowing the mixture to stand for 24 h. This hydroxide-based procedure dissolves only the organic portion of the material (linker and pore filling solvent), while the inorganic component of the MOF form zirconium hydroxide sinks to the bottom and is not measured. UV-vis spectra in both absorbance and reflectance mode, were collected on a Shimadzu UV-3600 spectrophotometer. The spectra were recorded in the 200−800 nm wavelength range. ^{1}H NMR spectra were recorded on Bruker Avance DPX-300 NMR Spectrometer (300 MHz). The relaxation delay (d_1) was set to 20 s to ensure that reliable integrals were obtained, allowing for the relative concentrations of the various organic species to be accurately determined. The number of scans was 64.

3. RESULTS AND DISCUSSION

3.1. Synthesis and Structure. The simplest way to prepare mixed linker−MOFs is to use a mixture of isostructural linkers of similar denticity and utilize them in a procedure closely resembling that used to obtain the nonfunctional analogue. Only a few examples in the literature follow such an approach: instead, most groups are optimizing the synthesis conditions specifically to obtain mixed-linker MOFs. Kleist et al.[26] have reported that the choice of reaction conditions plays a crucial role in the synthesis of mixed-linker MOFs based on the MOF-5 structure. Lammert et al.[30] also found that both the metal precursor and the solvent plays a key role in the synthesis of mixed-linker MOFs in the MIL-101 system. In this work on the UiO-66 topology, mixed-linker MOFs and phase-pure UiO-66 and UiO-66-NH_2 were successfully prepared under very similar synthesis conditions. The PXRD patterns of samples prepared with 25, 50, and 75 mol % ABDC are reported in Figure 1, clearly showing the crystalline nature of all the samples and perfectly matching with patterns of phase-pure UiO-66 and UiO-66-NH_2, confirming the synthesis of isostuctural mixed-linker frameworks with a face-centered cubic (FCC) structure.

Refinements of the PXRD patterns using the Pawley method (Accelyer Material Studio 6.6) show no significant change in the lattice parameter, decreasing from 20.77 Å to 22.74 Å when going from UiO-66 to UiO-66-NH_2. This very small change in the lattice constant and small size of crystallites (~100 nm, as determined by SEM) does not allow us to gather information on the distribution of linkers.

3.2. Quantitative Analysis of Linkers. Quantitative analysis of linkers in MOFs (in particular, ABDC) has been done by measuring the solutions obtained by disassembling the framework in an appropriate media. Although the disassembly of Zr-MOFs in 1 M NaOH was reported[15] before the recent development of fluoride-based media,[17] it had not been exploited further as a digestive media for quantitative analysis.

dx.doi.org/10.1021/ic500607a | Inorg. Chem. 2014, 53, 9509−9515

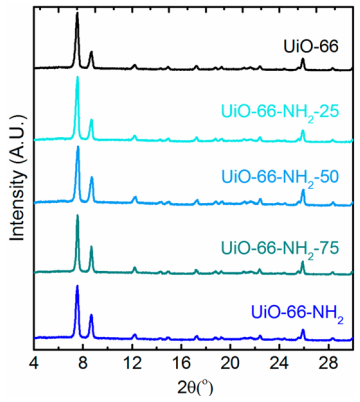

Figure 1. Comparison of the powder X-ray diffraction (PXRD) patterns of the mixed-linker MOF series. PXRD patterns up to 50° 2θ are given in Figure S1 in the Supporting Information.

The toxicity associated with fluoride-based media has led us to opt to continue working with 1 M NaOH solution for MOF disassembly. Moreover, the analysis (PXRD and TGA-DSC; see Figure S4 in the Supporting Information) of the undissolved solid obtained after the disassembly of the MOF in 1 M NaOH shows no signs of residual organic linker, which confirms that all of the linker present at the MOF is dissolved in solution.

DR-UV-vis spectroscopy measurements (see Figure S2 in the Supporting Information) provided a qualitative indication that the fraction of ABDC in the materials decreased in the order UiO-66-NH_2 > UiO-66-NH_2-75 > UiO-66-NH_2-50 > UiO-66-NH_2-25, as would be expected. This was evidenced by the decreasing intensity of a band at λ_{max} = 328 nm in the DR-UV−vis spectra. This band is assigned to the electronic transition from the nonbonding to antibonding molecular orbital of ABDC ($n \rightarrow \pi^*$) and is responsible for the yellow color of both the linker molecule and the MOFs that it forms.[34] In order to quantify the ABDC content with UV-vis spectroscopy, a calibration curve (inset of Figure 2) is required, allowing the Beer−Lambert law to be applied. The curve was obtained by recording the absorption spectra of standard solutions of ABDC of varying concentration in a 1 M NaOH media. The spectral absorbance at 328 nm was then plotted against the concentration. The absorbance spectra of the standard solutions are given in the Supporting Information (Figure S4).

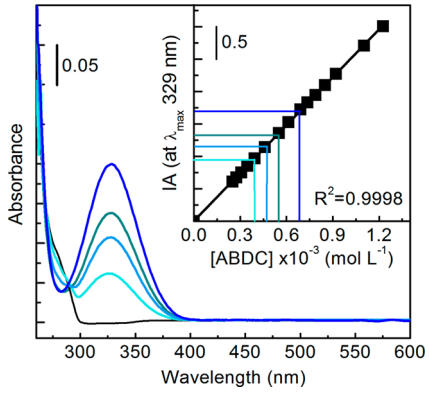

Figure 2. a) UV-vis absorbance spectra of MOFs disassembled in a 1 M aqueous NaOH solution for 24 h: UiO-66-NH_2, UiO-66-NH_2-75, UiO-66-NH_2-50, UiO-66-NH_2-25, and UiO-66. The inset shows the calibration curve obtained by plotting the integrated absorbance (IA) at λ_{max} = 329 nm of a standard solution of ABDC against concentration.

The concentration of ABDC in the MOFs can then be determined by measuring the absorption spectra on the digest solutions and interpolating the absorbance at 328 nm on the calibration curve. Table S2 in the Supporting Information details the method used to calculate the ABDC content in the mixed-linker MOFs using this data.

Providing a qualitative illustration of the results, Figure 3 shows the normalized ^{1}H NMR spectra obtained on the digestion solutions of all five samples in the series. As expected from the UV-vis data, when going through the series from UiO-66 to UiO-66-NH_2, the ABDC proton signal (3 × 1H, Figure 3b) systematically increases in intensity while the BDC proton signal (4H, Figure 3a) decreases. This result confirms that ABDC substitutes for BDC to an increasing extent throughout the series.

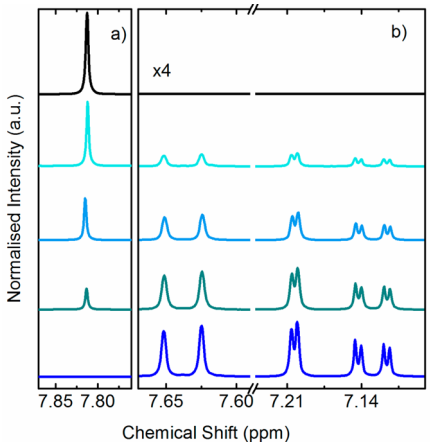

Figure 3. Normalized ^{1}H NMR spectra of the mixed-linker MOFs series digested for 24 h in a 1 M solution of NaOH in D_2O (UiO-66-NH_2, UiO-66-NH_2-75, UiO-66-NH_2-50, UiO-66-NH_2-25, and UiO-66): (a) proton signal associated with BDC and (b) signals associated with ABDC. Signals in panel b are multiplied by a factor of 4 for easy visual comparison of the signal intensities.

The quantitative analysis of these results (see section E of the Supporting Information for details of the method) affords the values presented in Table 1, alongside those of the UV-vis spectroscopy results. It can be seen that the values for ABDC content obtained by both spectroscopic methods are in satisfactory agreement. This validates the use of UV-vis spectroscopy applied to the quantitative analysis of ABDC containing mixed-linker MOFs. Furthermore, it is seen that the extent to which the substituted linker is incorporated into the

Table 1. ABDC Concentration Used in the Synthesis of Mixed-Linker MOFs, Compared with the ABDC Concentration Determined by UV-vis and NMR Spectroscopy

	[ABDC] [mol %]		
MOF	synthesis	UV-vis	NMR
UiO-66	0	0	0
UiO-66-NH_2-25	25	30	30
UiO-66-NH_2-50	50	54	57
UiO-66-NH_2-75	75	70	77
UiO-66-NH_2	100	104	100

dx.doi.org/10.1021/ic500607a | Inorg. Chem. 2014, 53, 9509−9515

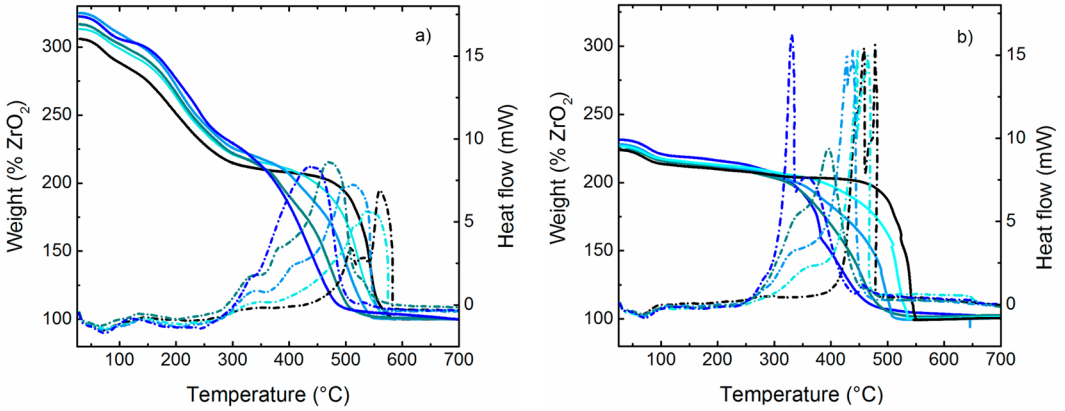

Figure 4. TG-DSC results of (a) as-prepared and (b) water-washed MOFs: UiO-66, UiO-66-NH_2-25, UiO-66-NH_2-50, UiO-66-NH_2-75, and UiO-66-NH_2. Solid lines represent TGA curves, while the DSC curves are dash-dotted. The end weight of the TGA run is normalized to 100% of ZrO_2, which is the expected product in the aerobic thermal decomposition of Zr-MOF.

crystalline product is almost the same as that expected by the ABDC:BDC ratio used in the synthesis mixtures. This was found not to be the case for another synthesis method where an excess of linker (ligand:metal ratio = 2:1) was used. There, the results indicated a clear preference for the nonfunctionalized BDC linker (see section G of the Supporting Information for more details).

3.3. Thermal Stability and Activation. Activation, which is the process of solvent removal from the pores of the framework, allows access to the porosity of the sample and thus is an important step in the development of MOFs for commercial applications as adsorbents and as catalysts.[21] Many MOFs are synthesized in dimethylformamide (DMF), which has a high boiling point and is strongly adsorbed inside the pores, especially so in MOFs with a high loading of polar functional groups, such as amines. The complete removal of such strongly adsorbed molecules usually requires high temperatures (ca. 250 °C) and the application of vacuum conditions, which cause many MOFs to decompose. This problem can be overcome by post-synthetically exchanging DMF with more-volatile solvents that do not affect the crystallinity of the samples.[21] In this work, activation was facilitated by the post-synthetic exchange of DMF with water, which is a procedure that has been proven to be very effective, especially in samples with high amino content. In order to investigate the effect that the ABDC content has on the thermal stability and activation of the frameworks, all five samples in the series were characterized by TGA, thermal treatments followed by PXRD, and Fourier transform infrared (FTIR) spectroscopy.

3.3.1. Thermogravimetric Analysis. Figures 4a and 4b present the TG-DSC results of the as-synthesized and water-exchanged samples, respectively. Three weight-loss steps are observed on the TGA curves of the as-synthesized samples. The initial weight loss of 5%−6% is observed up to 80 °C, while the second (25%−28%) is observed in the range of 100−280 °C. Such weight losses are due to the removal of solvent and the dehydroxylation of the zirconium oxo-clusters. The third and last weight loss step is due to the framework decomposition (T_{dec}) and occurs at a slightly different temperature on each.

In the case of UiO-66-NH_2, UiO-66-NH_2-75, and UiO-66-NH_2-50, this last step is not preceded by a clear plateau, indicating that the framework in fact starts to decompose before the solvent is totally removed. One last observation from the TGA curves is that there is a clear systematic increase in the decomposition temperature of the framework as the loading of ABDC in the framework decreases. A similar trend of stability has been observed in IRMOF-3/MOF-5-based mixed-ligand frameworks.[26] The DSC data reported in Figure 4a clearly indicates the exothermic nature of the framework decomposition, corresponding to the burning of linkers. In order to determine whether the mixed-linker MOF microcrystals studied in this work contain randomly distributed linker or are simply a physical mixture of pure UiO-66 and UiO-66-NH_2 MOFs phases, a separate TG-DSC experiment was performed on a physically mixed UiO-66 and UiO-66-NH_2 (molar ratio = 1:1) sample. These results are compared to that obtained on the UiO-66-NH_2-50 sample in Figure S8 in the Supporting Information. It is found that very little difference can be observed between the two samples, based on their TGA results; however, the DSC curves of the two measurements have clearly distinct profiles. In particular, the DSC curve of the physical mixture shows two well-separated heat signals at 430 °C (broad) and 490 °C (sharp), corresponding to the decomposition of the UiO-66-NH_2 and UiO-66 phases, respectively. In contrast, the decomposition of the UiO-66-NH_2-50 sample is signified by only a single, broad peak extending over a temperature range of 400−450 °C. This result provides convincing evidence that the linkers of the samples prepared here are indeed randomly distributed linker from crystal to crystal and are not just a physical mixture of the UiO-66 and UiO-66-NH_2 MOFs phases.

Figure 4b shows the TG-DSC results for the water-exchanged samples. Each MOF sample loses 5%−6% of their initial weight in the temperature range of 25−250 °C, and this is indicative of the removal of physisorbed water and the dehydroxylation of the zirconium oxo-clusters . This weight loss is very small, compared with the equivalent weight losses observed in the DMF containing as synthesized samples, suggesting that the DMF was removed very effectively by the water exchange procedure. Moreover, the solvent exchange seems to have had no effect on the decomposition temperature of the materials, such that the previously established relationship between the ABDC content and framework stability is maintained. The DSC curves of the water-washed samples suggest that the decomposition of the framework is more sharply defined and exothermic, when compared to the as-synthesized samples. This is likely due to the fact that the decomposition is no longer occurring simultaneously with the

dx.doi.org/10.1021/ic500607a | Inorg. Chem. 2014, 53, 9509−9515

endothermic solvent removal process, allowing the observation of the framework collapse as a much more precise exothermic event.

3.3.2. Infrared Spectroscopy. While TG-DSC profiles are very useful for following the behavior of samples during the heat treatments, and helping to identify suitable activation conditions, PXRD and FTIR are the techniques of choice for ensuring that the samples remain intact after the specific activation procedure. The full set of samples in the as-synthesized and water-washed forms, as well as after thermal treatment at 200 °C for 12 h in air, have been measured by both PXRD and DRIFT spectroscopy. The DRIFT results are displayed in Figure 5. Generally speaking, it is possible to follow

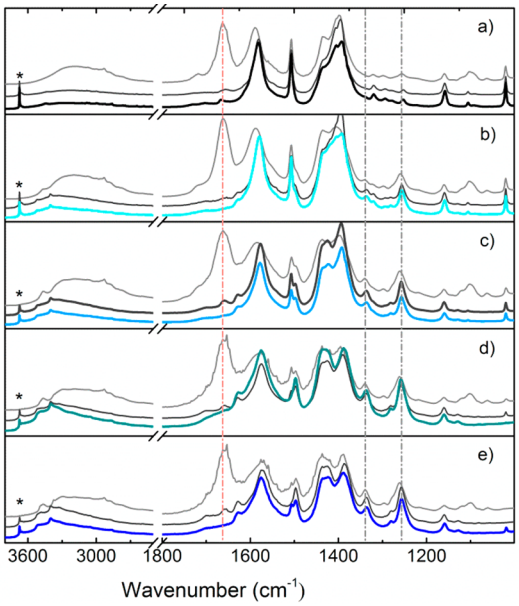

Figure 5. DRIFT spectra of UiO-66, part a; UiO-66-NH_2-25, part; UiO-66-NH_2-50, part c; UiO-66-NH_2-75, part d; and UiO-66-NH_2, part e. Three curves are shown for each spectrum, from top to bottom, represent the sample as-prepared (gray), water-washed (dark gray), and after heating for 12 h at 200 °C in air (same color code as in previous figures). DRIFT spectra were recorded on samples diluted with KBr. The pink and gray dash-dot lines mark the peaks associated with DMF and ABDC linker, respectively, while the asterisks show the absorption peaks associated with hydroxyl groups on the Zr clusters.

the solvent exchange and removal (progressive decreasing of specific fingerprint due to the solvent) and/or MOF framework decomposition (broadening of the bands below 1650 cm^{-1}. Other noteworthy observations from the DRIFT results are as follows:

(i) A strong absorption band at ~1665 cm^{-1} (dashed pink line), assigned to the ν(C═O) stretching of DMF, is seen only in the as synthesized samples. The absence of this band in the water-exchanged samples gives additional evidence for the complete exchange of DMF with water.[32]

(ii) Absorption bands at 1338 and 1261 cm^{-1} (dashed gray line, associated with ABDC) are seen to increase in intensity, as the ABDC content of the MOF increases.

(iii) The IR spectra collected after the thermal treatment show no broadening or weakening of the absorption bands, testifying that no dramatic change in the long-range order of the material has taken place.

This is backed up by the corresponding PXRD patterns shown in Figure S9 in the Supporting Information. The patterns show that all the samples retain high crystallinity, even after a prolonged thermal treatment. To our knowledge, such rigorous thermal stability tests (12 h treatment) previously have not been reported on any MOF.

3.3.3. N_2 Sorption. Nitrogen sorption isotherms measured at 77 K on the samples that were exchanged for water are shown in Figure 6. All the samples were heated at 200 °C for 2 h under vacuum prior to the adsorption of nitrogen.

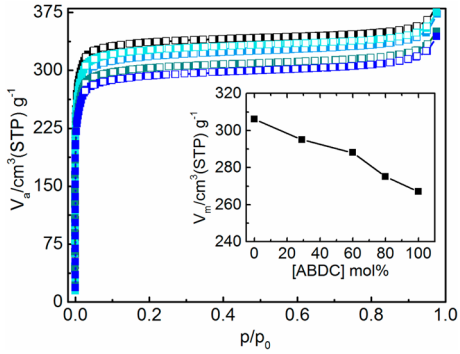

Figure 6. N_2 sorption isotherm at 77 K measured on water-washed samples of UiO-66, UiO-66-NH_2-25, UiO-66-NH_2-50, UiO-66-NH_2-75, and UiO-66-NH_2. The solid and open squares symbols represent the adsorption and desorption loop, respectively.

All the samples show type-I isotherms, confirming the microporous nature of the mixed-linker MOFs. The fully functionalized amino MOF is less porous than the parent UiO-66. This is as expected, since the NH_2 group will block some of the void space.[15] Moreover, the surface area and pore volume is observed to systematically decrease (inset Figure 6) as the ABDC content of the framework increases. Table 2 lists the

Table 2. Surface Areas and Pore Volumes of MOFs Calculated from the N_2 Sorption Isotherm at 77 K[a]

	Surface Area [m^2 g^{-1}]		
sample	BET	Langmuir	pore volume, V_m [cm^3(STP) g^{-1}]
UiO-66	1331	1444	306
UiO-66-NH_2-25	1284	1378	295
UiO-66-NH_2-50	1252	1361	288
UiO-66-NH_2-75	1198	1298	275
UiO-66-NH_2	1161	1254	267

[a]Prior to the N_2 adsorption, both samples were pretreated under vacuum for 1 h at 80 °C and for 2 h at 150 °C.

surface area (BET and Langmuir) and pore volumes of the samples calculated using the data in the p/p_0 range of 0−0.10 of the isotherm. All samples were found to remain intact after solvent removal, as evidenced by PXRD measurements performed on the materials following these N_2 adsorption measurements (see Figure S10 in the Supporting Information). While the addition of NH_2 functional groups reduces the internal volume, missing linkers will have the opposite effect. The surface area for the parent UiO-66 indicates that 3 of 24 linkers are missing.[39] Changes in linker ratio in the synthesis will probably also alter the amount of missing linkers

dx.doi.org/10.1021/ic500607a | Inorg. Chem. 2014, 53, 9509−9515

prohibiting a quantitative calculation of amine substitution based on absorption measurements alone.

3.4. Chemical Stability. The chemical stability of the series of materials was confirmed by measuring PXRD patterns before and after the treatment with aqueous (at room temperature (RT) and 100 °C), acidic (1 M HCl), and basic (1 M NaOH) media. Figure 7 shows the results of chemical stability tests on

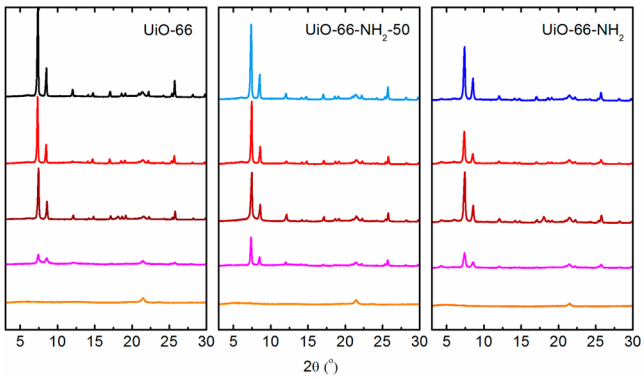

Figure 7. Powder XRD patterns of MOFs as prepared (with same color code used in previous figures), and after the treatment of 1 month in water (red), 24 h reflux in water (brown), 24 h in 1 M HCl (magenta), and 24 h in 1 M NaOH (orange).

UiO-66, UiO-66-NH_2-50, and UiO-66-NH_2 (see Figure S11 in the Supporting Information for the results on UiO-66-NH_2-25 and UiO-66-NH_2-75). The PXRD pattern obtained of the samples after the aqueous treatments (RT for 2 months and under reflux for 24 h) do not show any significant change. However, porosity of these samples, when refluxed in water for 24 h, show significant decrease (see Figure S12 in the Supporting Information). Interestingly, ABDC-functionalized MOFs were found to degrade more slowly than UiO-66 under acidic conditions, as previously reported by Krista and co-workers.[40] Of course, all samples undergo complete amorphization under basic conditions.

4. CONCLUSION

A series of mixed-linker metal−organic frameworks (MOFs) with UiO-66 topology have been successfully prepared using mixture of 2-aminobenzene-1,4-dicarboxylic acid (ABDC) and benzene-1,4-dicarboxylic acid (BDC). The thermal stability and porosity of the frameworks are significantly influenced by the ratio between ABDC and BDC in the framework. With this series, we have successfully demonstrated that UV-vis spectroscopy can be used for the quantitative determination of ABDC in mixed-linker MOFs. We have also demonstrated that 1 M NaOH can be used as a media for the disassembly of Zr-based MOFs for the quantitative analysis of linkers in amine-functionalized mixed-linker MOFs. By providing a method that allows control over the loading of the amino functionality, many opportunities for further studies on sorption and post-synthetic modifications are afforded.

■ ASSOCIATED CONTENT

Supporting Information

Synthetic details, methods of quantitative analysis of ABDC by UV−visible and ^{1}H NMR spectroscopy, key results for materials prepared with modified reaction conditions, TG-DSC comparison of physical mixture and UiO-66-NH_2-50, and thermal treatments followed by PXRD. This material is available free of charge via the Internet at http://pubs.acs.org.

■ AUTHOR INFORMATION

Corresponding Authors

*E-mail: sachin.chavan@kjemi.uio.no, chasachin@gmail.com (S. M. Chavan).

*E-mail: silvia.bordiga@kjemi.uio.no, silvia.bordiga@unito.it(S. Bordiga).

Notes

The authors declare no competing financial interest.

■ ACKNOWLEDGMENTS

The Research Council of Norway (CLMIT Project No. 215735), VISTA (Project No. 6457), and MIUR-PRIN 2010-2011 (Project No. 2010A2FSS9) are kindly acknowledged for the financial support. We thank Sharmala Aravinthan for her help in material synthesis and characterization.

■ REFERENCES

(1) Eddaoudi, M.; Moler, D. B.; Li, H. L.; Chen, B. L.; Reineke, T. M.; O'Keeffe, M.; Yaghi, O. M. *Acc. Chem. Res.* **2001**, *34* (4), 319.
(2) Yaghi, O. M.; O'Keeffe, M.; Ockwig, N. W.; Chae, H. K.; Eddaoudi, M.; Kim, J. *Nature* **2003**, *423* (6941), 705.
(3) Kitagawa, S.; Kitaura, R.; Noro, S. *Angew. Chem., Int. Ed.* **2004**, *43* (18), 2334.
(4) Ferey, G. *Chem. Soc. Rev.* **2008**, *37* (1), 191.
(5) Morris, R. E.; Wheatley, P. S. *Angew. Chem., Int. Ed.* **2008**, *47* (27), 4966.
(6) Li, J. R.; Sculley, J.; Zhou, H. C. *Chem. Rev.* **2012**, *112* (2), 869.
(7) Farrusseng, D.; Aguado, S.; Pinel, C. *Angew. Chem., Int. Ed.* **2009**, *48* (41), 7502.
(8) Lee, J.; Farha, O. K.; Roberts, J.; Scheidt, K. A.; Nguyen, S. T.; Hupp, J. T. *Chem. Soc. Rev.* **2009**, *38* (5), 1450.
(9) Corma, A.; Garcıa, H.; Llabres i Xamena, F. X. *Chem. Rev.* **2010**, *110* (8), 4606.
(10) Cunha, D.; Ben Yahia, M.; Hall, S.; Miller, S. R.; Chevreau, H.; Elkaim, E.; Maurin, G.; Horcajada, P.; Serre, C. *Chem. Mater.* **2013**, *25* (14), 2767.
(11) Cunha, D.; Gaudin, C.; Colinet, I.; Horcajada, P.; Maurin, G.; Serre, C. *J. Mater. Chem. B* **2013**, *1* (8), 1101.
(12) Wang, Z.; Tanabe, K. K.; Cohen, S. M. *Inorg. Chem.* **2008**, *48* (1), 296.
(13) Cohen, S. M. *Chem. Rev.* **2011**, *112* (2), 970.
(14) Gascon, J.; Aktay, U.; Hernandez-Alonso, M. D.; van Klink, G. P. M.; Kapteijn, F. *J. Catal.* **2009**, *261* (1), 75.
(15) Kandiah, M.; Nilsen, M. H.; Usseglio, S.; Jakobsen, S.; Olsbye, U.; Tilset, M.; Larabi, C.; Quadrelli, E. A.; Bonino, F.; Lillerud, K. P. *Chem. Mater.* **2010**, *22* (24), 6632.
(16) Vermoortele, F.; Ameloot, R.; Vimont, A.; Serre, C.; De, V. D. *Chem. Commun.* **2011**, *47* (5), 1521.
(17) Roy, P.; Schaate, A.; Behrens, P.; Godt, A. *Chem.—Eur. J.* **2012**, *18* (22), 6979.
(18) Yang, Q. Y.; Wiersum, A. D.; Llewellyn, P. L.; Guillerm, V.; Serred, C.; Maurin, G. *Chem. Commun.* **2011**, *47* (34), 9603.
(19) Cmarik, G. E.; Kim, M.; Cohen, S. M.; Walton, K. S. *Langmuir* **2012**, *28* (44), 15606.
(20) Sumida, K.; Rogow, D. L.; Mason, J. A.; McDonald, T. M.; Bloch, E. D.; Herm, Z. R.; Bae, T. H.; Long, J. R. *Chem. Rev.* **2012**, *112* (2), 724.
(21) Farha, O. K.; Hupp, J. T. *Acc. Chem. Res.* **2010**, *43* (8), 1166.
(22) Burrows, A. D. *CrystEngComm* **2011**, *13* (11), 3623.
(23) Das, M. C.; Xiang, S. C.; Zhang, Z. J.; Chen, B. L. *Angew. Chem., Int. Ed.* **2011**, *50* (45), 10510.
(24) Bunck, D. N.; Dichtel, W. R. *Chem.—Eur. J.* **2013**, *19* (3), 818.
(25) Foo, M. L.; Matsuda, R.; Kitagawa, S. *Chem. Mater.* **2013**, *26* (1), 310.

(26) Kleist, W.; Maciejewski, M.; Baiker, A. *Thermochim. Acta* **2010**, *499* (1−2), 71.
(27) Marx, S.; Kleist, W.; Huang, J.; Maciejewski, M.; Baiker, A. *Dalton Trans.* **2010**, *39* (16), 3795.
(28) Lescouet, T.; Kockrick, E.; Bergeret, G.; Pera-Titus, M.; Aguado, S.; Farrusseng, D. *J. Mater. Chem.* **2012**, *22* (20), 10287.
(29) Reinsch, H.; Waitschat, S.; Stock, N. *Dalton Trans.* **2013**, *42* (14), 4840.
(30) Lammert, M.; Bernt, S.; Vermoortele, F.; De Vos, D. E.; Stock, N. *Inorg. Chem.* **2013**, *52* (15), 8521.
(31) Cavka, J. H.; Jakobsen, S.; Olsbye, U.; Guillou, N.; Lamberti, C.; Bordiga, S.; Lillerud, K. P. *J. Am. Chem. Soc.* **2008**, *130* (42), 13850.
(32) Valenzano, L.; Civalleri, B.; Chavan, S.; Bordiga, S.; Nilsen, M. H.; Jakobsen, S.; Lillerud, K. P.; Lamberti, C. *Chem. Mater.* **2011**, *23* (7), 1700.
(33) Kim, M.; Cohen, S. M. *CrystEngComm* **2012**, *14* (12), 4096.
(34) Chavan, S.; Vitillo, J. G.; Gianolio, D.; Zavorotynska, O.; Civalleri, B.; Jakobsen, S.; Nilsen, M. H.; Valenzano, L.; Lamberti, C.; Lillerud, K. P.; Bordiga, S. *Phys. Chem. Chem. Phys.* **2012**, *14* (5), 1614.
(35) Wang, Z. Q.; Cohen, S. M. *Chem. Soc. Rev.* **2009**, *38* (5), 1315.
(36) Kandiah, M.; Usseglio, S.; Svelle, S.; Olsbye, U.; Lillerud, K. P.; Tilset, M. *J. Mater. Chem.* **2010**, *20* (44), 9848.
(37) Ranocchiari, M.; Lothschuetz, C.; Grolimund, D.; van Bokhoven, J. A. *Proc. R. Soc. A* **2012**, *468* (2143), 1985.
(38) Kim, M.; Cahill, J. F.; Prather, K. A.; Cohen, S. M. *Chem. Commun.* **2011**, *47* (27), 7629.
(39) Shearer, G. C.; Chavan, S.; Ethiraj, J.; Vitillo, J. G.; Svelle, S.; Olsbye, U.; Lamberti, C.; Bordiga, S.; Lillerud, K. P. *Chem. Mater.* **2014**, *26*, 4068−4071.
(40) DeCoste, J. B.; Peterson, G. W.; Jasuja, H.; Glover, T. G.; Huang, Y. G.; Walton, K. S. *J. Mater. Chem. A* **2013**, *1* (18), 5642.

dx.doi.org/10.1021/ic500607a | *Inorg. Chem.* 2014, 53, 9509−9515